

The Non-Negative Mode Theorem in False Vacuum Decay with Gravity

Takahiro Tanaka

Department of Earth and Space Science, Graduate School of Science
Osaka University, Toyonaka 560-0043, Japan

The so-called negative mode problem in the path integral approach to the false vacuum decay with the effect of gravity has been an unsolved problem. Several years ago, we proposed a conjecture which is to be proved in order to give a consistent solution to the negative mode problem. We called it the 'no-negative mode conjecture'. In the present paper, we give a proof of this conjecture for rather general models. Recently, we also proposed the 'no-supercritical supercurvature mode conjecture' that claims the absence of supercritical supercurvature modes in the one-bubble open inflation model. In the same paper, we clarified the equivalence between the 'no-negative mode conjecture' and the 'no-supercritical supercurvature mode conjecture'. Hence, the latter is also proved at the same time when the former is proved.

I. INTRODUCTION

In recent years, the process of the false vacuum decay with the effect of gravity has been studied extensively in the context of the one-bubble open inflation scenario, in which an open universe is created in a nucleated bubble formed through false vacuum decay [1]. In this context, we are interested in the spectrum of quantum fluctuations after the bubble nucleation because it determines the spectrum of primordial fluctuations of the universe. By comparing the predicted spectrum with the observed one, we can test whether a certain model is viable or not. The fluctuation can be decomposed by using the spatial harmonics in an open universe. We denote the eigen value of the spatial harmonics by p^2 . The spatial harmonics with positive p^2 are square integrable on a time constant hypersurface in an open universe, and we have a continuous spectrum for $p^2 > 0$. While, the spatial harmonics are no longer square integrable when the eigen value p^2 is negative. However, since any time constant hypersurface in an open universe is not a Cauchy surface, this divergence does not directly prohibit the existence of such a mode. By considering the normalization of perturbation modes on an appropriate Cauchy surface, we find that the spectrum for $p^2 < 0$ can exist as a discrete one, which we call supercurvature mode [2].

Further, we classified the modes with negative p^2 into two classes depending on their eigen values. One is supercritical modes with $p^2 < -1$ and the other is subcritical modes with $p^2 > -1$. If and only if there exist supercritical modes, the two-point correlation function of the tunneling field unboundedly increases for large spatial separation in the open universe created in the nucleated bubble. The diverging correlation for large spatial separation does not seem to be allowed intuitively. Hence, we proposed the 'no-supercritical supercurvature mode conjecture', which is the conjecture claiming that the existence of supercritical supercurvature modes should be

prohibited in realistic models of creation of an open universe [3].

On the other hand, there is an unsolved problem in the Euclidean path integral approach to describe the phenomena of the true vacuum bubble nucleation with the effect of gravity through quantum tunneling [4]. That is the so-called negative mode problem [5]. In the lowest WKB approximation, the quantum tunneling is described by a bounce solution [5,6]. The decay rate per unit volume and per unit time interval, Γ , is given by the formula

$$= \text{Im} (K) e^{(S_E^{(\text{bounce})} - S_E^{(\text{trivial})})}; \quad (1.1)$$

where $S_E^{(\text{bounce})}$ is the classical Euclidean action for the bounce solution and $S_E^{(\text{trivial})}$ is that for the trivial solution that stays in the false vacuum. In the path integral approach, the prefactor $\text{Im} (K)$ is evaluated by taking the imaginary part of the gaussian integral over fluctuations around the background bounce solution. For an ordinary system without gravity, there is one perturbation mode in which direction the action does not decrease. It is called negative mode. The existence of an unique negative mode has already proved for quantum fields in flat spacetime [7]. In evaluating this gaussian integral, the path of integration is deformed on the complex plane to make the integral well-defined. As a result, one imaginary factor, i , appears in K . In the Euclidean path integral approach to the tunneling, this imaginary unit plays a crucial role when we interpret Γ as the decay rate.

However, in the case where gravity is taken into account, the situation is different. In this case, the tunneling is described by the $O(4)$ -symmetric Coleman and De Luccia (CD) bounce solution [8]. In reducing the action for fluctuations around the $O(4)$ -symmetric CD bounce solution, we used the standard gauge fixing method to deal with gauge degrees of freedom [9]. Then, we obtained the reduced action that retains only the physical degrees of freedom [4,10]. Regarding the fact that

the action with gravitational degrees of freedom is unbounded below, the reduced action for the fluctuations that conserve the $O(4)$ -symmetry has an unusual overall signature. To treat this system, we proposed to use the prescription similar to the conformal rotation [4,14]. Then, from path integral measure, there arise one imaginary unit i . Hence, in order to obtain a correct number of i , i.e., one, it seems that there should exist no-negative mode. Therefore, we proposed the 'no-negative mode conjecture'.

We have shown in our previous paper [3] that the existence of supercritical supercurvature modes is equivalent to the existence of negative modes. That is, if we obtain a proof of the 'no-negative mode conjecture', the 'no-supercritical supercurvature mode conjecture' is also proved. Hence, the issue if the 'no-negative mode conjecture' is true or not is now of increasing importance. In the same paper [3], we have shown that this conjecture holds in a certain restricted situation. In the present paper, we give a proof of this conjecture for rather general models which consist of one scalar field.

Here, we briefly describe the statement proved in the present paper. Here, we should note that not all CD bounce solutions contribute to the tunneling process. The relevant contribution to the decay rate comes only from the bounce solution that realizes the minimum value of action among all non-trivial solutions. Thus, the statement that we should prove is the following: 'There is no-negative mode for the CD bounce solution that realizes the minimum value of action among all non-trivial solutions.'

However, making a list of all the CD bounce solutions, we find that there are many solutions for which the tunneling field does not change monotonically. These solutions have more than two concentric domain walls. We expect that the simplest bounce solution with one domain wall dominate the tunneling process. Hence, one may want to strengthen the conjecture as follows: For the bounce solution that gives the minimum value of action, the tunneling field changes monotonically, and this solution have no-negative mode. We refer to this version of conjecture as the 'no-negative mode theorem'. We used the word 'theorem' instead of 'conjecture' because this statement is proved in this paper.

This paper is organized as follows. In section II, we explain the 'no-negative mode theorem' in more detail. In section III, we present a prescription to search for all CD bounce solutions. In section IV, we give a method to count the number of negative modes for a given CD bounce solution. In section V, we give a method to count the multiplicity of domain walls contained in a given solution. In section VI, we give a method to compare the values of action between various CD bounce solutions for a given potential model. In Section VII, combining the results obtained in Sec. IV, V and VI, we prove the 'no-negative mode theorem'. We summarize the outline of the proof and discuss the implication of this theorem in section VIII.

II. STATEMENT TO BE PROVED

In this section, we explain the statement, which we call the 'no-negative mode theorem', in more detail to clarify what we are going to prove.

We consider the system composed of a scalar field, with the Einstein gravity. The Euclidean action is given by

$$S_E = \int d^4x \frac{1}{2}g^{-1}R + \frac{1}{2}g^{\mu\nu}\partial_\mu\Phi\partial_\nu\Phi + V(\Phi); \quad (2.1)$$

where $\Phi = 8G$ and R is the Ricci curvature. The potential of the scalar field is assumed to have the form as shown in Fig.1, and initially the field is trapped in the false vacuum. We set $\Phi = 0$ at the top of the potential barrier and we denote the bottom in the false and true vacua by Φ_- and Φ_+ , respectively. We assume that $dV/d\Phi$ vanishes only at $\Phi_+, 0$ and Φ_- .

The bounce solution is an Euclidean solution which connects the configurations before and after tunneling. In the present case, before tunneling the geometry is given by the de Sitter space and the scalar field is in the false vacuum. After tunneling, there appears a true vacuum bubble in the false vacuum sea. Under the assumption of the $O(4)$ -symmetry,

$$ds^2 = N^2(\Phi)d\Phi^2 + a^2(\Phi)d\theta^2 + \sin^2\theta d\phi^2; \quad (2.2)$$

the corresponding bounce solution is found by Coleman and De Luccia [8]. With this assumption, the Euclidean action reduces to

$$S_E = 2^{-2}\int d\Phi N a^3 \left[\frac{1}{2N^2} \dot{\Phi}^2 + V(\Phi) \right] - \frac{3}{N^2} \frac{H^2}{a^2} + \frac{1}{a^2}; \quad (2.3)$$

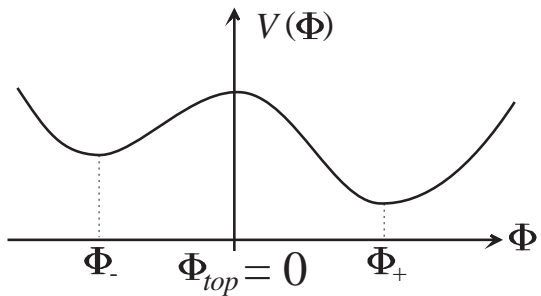


FIG.1. A typical shape of a tunneling field potential under consideration. We assume that the potential take its extrema only at Φ_+ and Φ_- .

where $_$ represents the differentiation with respect to $_$ and $H = a = a$. Here $_$ is the value of $_$ at both boundaries. We assume that $_ > 0$ and $_ < 0$. For definiteness, we assume that $_$ is in the true (false) vacuum side at $_ = +$ ($_ = -$). Due to this restriction, we do not take account of solutions in which $_$ is in the same vacuum side at both boundaries.

The Euclidean equations of motion are obtained by taking the variation of S_E . After taking variations, we adopt the synchronous gauge by setting $N = 1$, for simplicity. The differentiation with respect to N gives a constraint equation,

$$H^2 - \frac{1}{a^2} = \frac{1}{3} \frac{1}{2} _^2 - V(_) : \quad (2.4)$$

From the variation with respect to $_$ and a , we obtain the equations of motion,

$$+ 3H - \frac{dV(_)}{d_] = 0; \quad (2.5)$$

$$H + \frac{1}{a^2} = - \frac{1}{2} _^2; \quad (2.6)$$

where we also used the constraint equation (2.4) to write the equation in the form as given in (2.6). We refer to the above two equations, (2.5) and (2.6), as the background equations. Requiring the regularity at both boundaries, the boundary conditions to be satisfied by the background solutions are determined as

$$-! 0; a ! j \quad j \quad (\text{for } ! \quad): \quad (2.7)$$

Recently, Hawking and Turok proposed to relax these boundary conditions to allow singular instantons [11]. However, the interpretation of singular instantons is still an unsettled issue [12]. Here we do not consider this possibility.

Now, we consider fluctuations around this bounce solution, to examine the prefactor K that arises in the estimate of the decay rate. As briefly noted in Introduction, the number of i in the prefactor K is important in the path integral approach. To evaluate the number of i , we need to obtain the reduced action for the fluctuations around the bounce solution. Especially, $O(4)$ -symmetric perturbations

$$\begin{aligned} ds^2 &= (1 + 2A(_)) d^2 \\ &\quad + a^2 (1 + 2H_L(_)) d^2 + \sin^2 d^2; \\ &= + (_); \end{aligned} \quad (2.8)$$

are most important. After an appropriate gauge fixing, we obtain the reduced action for $O(4)$ -symmetric perturbations as [4,10]

$${}^{(2)}S = \frac{3}{2} \int d_] i \frac{dq}{d_] + \frac{1}{2} (_^2 + \frac{1}{2} (U - 3)q^2); \quad (2.9)$$

with the potential U ,

$$U = \frac{1}{2} \frac{_^2}{a^2} - \frac{3}{a} + 2 \frac{a}{_} + \frac{a^2}{_^2}; \quad (2.10)$$

where q is the $O(4)$ -symmetric part of the gauge invariant variable introduced in Ref. [10], and $_^q$ is its conjugate momentum. The Euclidean conformal time $_$ is related to $_$ by $d_] = d_ = a(_)$. As given in Ref. [10], perturbations in terms of original variables are written down in the Newton gauge as

$$A = \frac{^0q}{2a}; \quad H_L = - \frac{^0q}{2a}; \quad = \frac{1}{a} \frac{d(^0q)}{d_]}; \quad (2.11)$$

where 0 denotes the differentiation with respect to $_$.

A distinguishable feature of the reduced action for $O(4)$ -symmetric perturbations is that the coefficient in front of $(_^q)^2$ becomes negative. Note that the prefactor K is evaluated by

$$K = \int d_] q dq e^{{}^{(2)}S}; \quad (2.12)$$

Thus, in doing the integration with respect to momentum variables, we will find that the gaussian integral does not converge. To resolve this difficulty, we proposed to use the prescription similar to the conformal rotation [4,14]. By changing the variables like $_^q = i^q, q = iq$, the above integration becomes well-defined. If we discretize the path integral, the numbers of $_^q$ and q integrations are different by 1. Therefore, this change of variable will produce one imaginary unit i . That is,

$$\begin{aligned} K &= \int d_] q dq e^{{}^{(2)}S} \\ &= \int d_] q \exp \left(\frac{3}{2} \int d_] \left(\frac{1}{2} \frac{dq}{d_]^2 + \frac{1}{2} (U - 3)q^2 \right) \right); \end{aligned} \quad (2.13)$$

To determine the number of i in K , we also need to know the spectrum of eigen values, $_j$, of the following Schrodinger type equation:

$$\frac{d^2}{d_]^2} + U - 3 q_j^2 = - _j q_j; \quad (2.14)$$

The contribution to K from $O(4)$ -symmetric perturbations will be given by $\int d_] q_j^2 e^{{}^{(2)}S}$. If there is no mode which has a negative eigen value, there arises no additional imaginary unit factor. Then, the prefactor K becomes imaginary. Thus, we conjectured that there should not be any negative mode for the system including the gravitational degrees of freedom, in Ref. [4]. As discussed in Ref. [3,4], one can show that, if there is no-negative mode in $O(4)$ -symmetric perturbations, it is also the case for the other perturbation modes. Hence, it is sufficient to concentrate on $O(4)$ -symmetric perturbations.

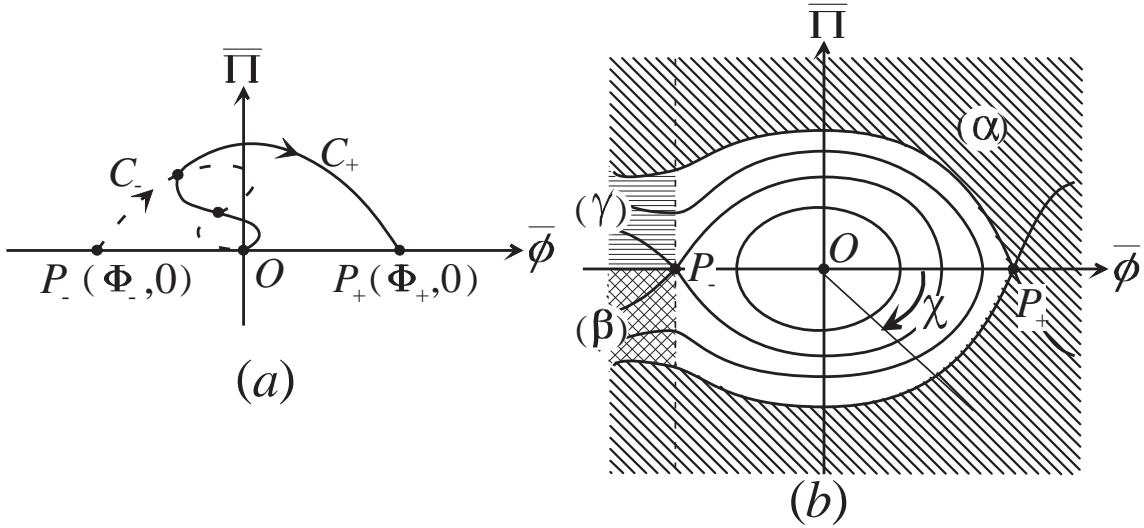


FIG. 2. (a) A schematic plot of $(\Pi; \phi)$. (Π) and (ϕ) are the values of $(\Pi; \phi)$ and its conjugate evaluated at the maximum radius. $(\Pi; \phi)$ is obtained by solving the background equations with the regular boundary condition at $\phi = 0$, where $a = 0$. The direction of the curves C is determined so that ϕ , the initial value of ϕ , increases along the curves. (b) The thick curves are ϕ -constant contours. The curves C do not enter the shaded regions labeled with (α) and (β) . Also in this figure, the angular coordinate χ is introduced. Note that χ increases in the clockwise direction.

As we have shown in Ref. [3], we can construct models of CD bounce solutions which possess negative modes. Hence, we cannot prove the absence of negative modes for arbitrary models of CD bounce solutions. However, as mentioned in Introduction, the important point is that not all CD bounce solutions contribute to the tunneling process. The bounce solution that determines the decay rate is the one that realizes the minimum value of action among all bounce solutions. Here, we strictly define the "no-negative mode theorem", a proof of which we are going to present in this paper.

The Main Theorem (the no-negative mode theorem): For the CD bounce solution that realizes the minimum value of action among all non-trivial solutions, Π^0 has a definite signature and the eigen value equation, Eq.(4.1), has no negative eigen modes.

III. A NEW METHOD TO FIND ALL $O(4)$ -SYMMETRIC CD BOUNCE SOLUTIONS

We develop a method to construct a complete list of $O(4)$ -symmetric CD bounce solutions in this section. For this purpose, we introduce a diagram consisting of two curves. We show that each intersection point of these curves corresponds to a CD bounce solution.

In solving the background equations, if we fix the boundary value of ϕ at one side, say $\phi = \phi_+$ at $\Pi = 0$, the boundary conditions (2.7) completely determines the initial condition to solve the equations of motion, (2.5) and (2.6). Then, solving Eqs. (2.5) and (2.6) from both sides to the maximum radius, we obtain functions which

satisfy the background equations in the respective half Euclidean regions. We denote them by

$$(\Pi^i; \phi); \quad a(\Pi^i; \phi); \quad (3.1)$$

where the subscript $+$ ($-$) is attached with the variables that are used in solving the background equations from the true (false) vacuum side. When we solve the background equations from $\phi = \phi_+ (> 0)$, the initial condition is varied by sweeping Π^i_+ between the true vacuum minimum and the top of the potential, i.e., $\Pi^i_0 = 0$ to Π^i_+ . While, when we solve them from $\phi = \phi_- (< 0)$, Π^i_0 is swept between the false vacuum minimum and the top of the potential, i.e., $\Pi^i_0 = 0$.

Here, we move the origin of the ϕ -coordinate to the point corresponding to the maximum radius, i.e., $a(\Pi^i; 0) = 0$. Thus, ϕ is determined by solving $a(\Pi^i; \phi) = 0$, and becomes a function of Π^i . Further, we define two functions of Π^i by the values of ϕ and $\Pi^i = 2^2 a^3 -$ at $\phi = 0$. We refer to them as (Π^i) and (Π^i) , respectively, where the subscript i is used in the same manner as before.

Then, as shown in Fig 2(a), the points $(\phi_+ (\Pi^i_+); \Pi^i_+)$ and $(\phi_- (\Pi^i_-); \Pi^i_-)$ draw two curves, C_+ and C_- , on the (Π, ϕ) -plane as Π^i_+ and Π^i_- are swept. Since $(\Pi^i; \phi)$ stays at $\phi = 0$ when $\Pi^i = 0$ or $\Pi^i = \Pi^i_0$, the curve C_- starts from $P_- = (\Pi^i_0; 0)$ and terminates at $O = (\Pi^i_0 = 0; 0)$ and the curve C_+ starts from O and terminates at $P_+ = (\Pi^i_+; 0)$. We refer to the curves moving in the opposite direction as (C) .

Proposition 1: Each of the curves C does not inter-

sect with itself .

Proof. If it were the case, we would have the same final values of and $\dot{a} = 0$ for different solutions. However, the background equations can be solved reversely from $\dot{a} = 0$, and the evolution is uniquely determined. This is a contradiction. \square

Proposition 2: All intersection points between C_+ and C_- correspond to CD bounce solutions. (An exceptional case is the Hawking Moss instanton corresponding to $i = 0$ [13];)

Proof. We set $(\dot{a}(\tau); a(\tau)) = (\dot{a}_+(\tau); a_+(\tau))$ for $\tau < 0$ and $(\dot{a}(\tau); a(\tau)) = (\dot{a}_-(\tau); a_-(\tau))$ for $\tau > 0$. Then, the values and the first derivatives of $a(\tau)$ are continuous at $\tau = 0$ for intersection points. With the aid of Eq.(2.4) we find that $a(\tau)$ is also continuous at $\tau = 0$. Since $(\dot{a}_+(\tau); a_+(\tau))$ and $(\dot{a}_-(\tau); a_-(\tau))$, respectively, satisfy the regular boundary conditions at $\tau = +$ and at $\tau = -$, $(\dot{a}(\tau); a(\tau))$ satisfies those at both boundaries. Hence, $(\dot{a}(\tau); a(\tau))$ is a CD bounce solution. \square

Before closing this section, we show that there is another general constraint on C . We define a function

$$(\tau) = \frac{1}{2} \tau - \frac{1}{3} \tau^3 - \frac{2}{3} \tau^2 \quad V(\tau) = \frac{1}{2a^6} \tau^2 - V(\tau); \quad (3.2)$$

where we used Eq.(2.4) with $H = 0$. As a function of τ and i , the definition of τ is implicit. To determine τ from this equation, we need to solve a third order algebraic equation like $\tau^3 + \tau^2 + \tau = 0$, where τ and i are real. The left hand side of this equation is a monotonic function of τ , and hence the real solution for τ is unique. We schematically plot the τ -constant contours in Fig.2(b). From Eq. (2.5), we can see that $E(\tau) = (1=2)^2 V(\tau)$ decreases monotonically in the direction for τ to increase. Thus, $\tau = (\tau; i) = E(0)$ is bounded by

$$\tau < E(\tau) = V(\tau^i) < V(\tau); \quad (\text{for } C_-); \quad (3.3)$$

Proposition 3: The curves C do not enter the shaded regions labeled with (τ) and (τ) in Fig.2(b).

Proof. It is manifest that C cannot go into the regions (τ) and (τ) in Fig.2(b) from the bound (3.3). On the other hand, from (3.3) alone, it seems possible that the

curve C_+ enters into the region (τ) . However, for the potential that we assumed, $dV(\tau)/d\tau$ stays negative once τ becomes smaller than τ . Hence, when we solve equations of motion from $\tau = +$, τ never stops on the left side of τ . Therefore, when $\tau < \tau$, τ must be positive. \square

For the later convenience, we introduce a new coordinate, $(\tau; i)$, where τ is given by (3.2) and i is defined by

$$(\cos \tau; \sin \tau) = \frac{(\tau; i)}{\sqrt{\tau^2 + i^2}}; \quad (3.4)$$

for the unshaded region in Fig.2(b). For the region (τ) , which the curve C_+ can enter, we extend the τ -coordinate so that it changes monotonically along each τ -constant curve and does not have a point with $\tau = m$ in this region, where m is an integer.

IV. NUMBER OF NEGATIVE MODES

In this section, we develop a method to count the number of negative modes of Eq. (2.14) from the topology of the $(\tau; i)$ -diagram introduced in the preceding section. Unless i^0 goes to 0, Eq. (2.14) is a Schrödinger type equation with a regular potential. In this case, the number of nodes of q_j for $j = 0$ gives the number of negative modes. Hence, as long as such nodeless bounce solutions are concerned, we can say that there is no-negative mode when q_j for $j = 0$ has no node. Therefore, we concentrate on the case with $j = 0$. Although the above statement does not hold any longer once a node of i^0 appears, we do not assume $i^0 \neq 0$ in most of the following discussions in this section. The only exception is the subsection C.

In subsection A, we introduce variables $q(\tau)$ defined by Eq.(4.1) with Eq.(4.2). They are constructed from the background solution $(\dot{a}^i(\tau); i)$, and we show that they satisfy Eq. (2.14) for $j = 0$ with $i = i^0$. Then, in subsection B, we give a method to count the number of nodes of the functions $x = (-q)$ from the $(\tau; i)$ -diagram. Further, we define a topological number N assigned for each intersection point, and show that it should be non-negative. In subsection C, we prove the following Theorem .

Theorem 1:

For an $O(4)$ -symmetric CD bounce solution which does not have a point at which $i^0 = 0$, the number of negative modes is given by N defined by Eq.(4.23). (See also the remark given at the end of this section.)

Define curves C^0 and C_+^0 by connecting points $(\tau^i; i)$, $(\tau^i; i)$ and $(\tau^i; i)$, $(\tau^i; i)$, respectively. By the same reasoning, we can also prove that C_- does not intersect with C^0 .

A. construction of a zero mode solution

We begin this subsection by pointing out that Eq. (2.14) for $j = 0$ is nothing but the perturbed equations of motion that are obtained by taking the variation of the reduced action. Since the $O(4)$ -symmetry is the symmetry that the background solution possesses, it is natural to consider that the case with $j = 0$ is related to the background solutions.

Proposition 4: We define functions q_+ and q_- by

$$q = \frac{a^2}{3} - \frac{'}{'} - \frac{''}{''}; \quad (4.1)$$

where

$$' = \frac{\partial}{\partial} \left(\frac{a^2}{3} \right); \quad (4.2)$$

Then, q_+ and q_- satisfy Eq. (2.14) for $j = 0$ with $\psi = 0$ regular boundary conditions.

Proof. First, we derive the equation satisfied by $'$. Hereafter, we sometimes suppress the subscript i to keep the simplicity of notation. It is obtained by differentiating the background equations with respect to a^i . From Eq.(2.5), we have

$$' + 3 \frac{\partial H}{\partial a^i} - + 3H \frac{'}{'} - \frac{d^2 V}{d^2} \frac{'}{'} = 0; \quad (4.3)$$

From Eqs.(2.4) and (2.6), we have

$$H - + H^2 = - \frac{2}{3} + V : \quad (4.4)$$

Differentiating this equation with respect to a^i , we obtain

$$\frac{d}{d} \left(\frac{\partial H}{\partial a^i} \right) + 2H \frac{\partial H}{\partial a^i} = - \frac{2}{3} - + \frac{dV}{d} : \quad (4.5)$$

By eliminating $\partial H / \partial a^i$ from Eqs. (4.3) and (4.5), we obtain a third-order differential equation with respect to $'$. After a lengthy but straightforward calculation, one can verify that the equation that $'$ satisfies reduces to

$$\frac{d^2}{d^2} + U - 3 \frac{a^2}{3} - \frac{'}{'} - \frac{''}{''} = 0; \quad (4.6)$$

where we used the relation

$$\frac{H}{2} = H - + \frac{1}{a^2} - - + \frac{H}{a^2} : \quad (4.7)$$

From Eq.(4.6), it is manifest that q defined by (4.1) satisfies Eq. (2.14) for $j = 0$ with $\psi = 0$. We note that q is defined not only for intersection points corresponding to CD bounce solutions but also for any points on the curves C .

Next, we show that q satisfies the required boundary condition, i.e., $q \rightarrow 0$ for $a \rightarrow \infty$. From the boundary condition for the background solutions, we have

$$a^i \frac{1}{2} c_1 \left(\frac{a^i}{a} \right)^2; \\ a^i c_2 \left(\frac{a^i}{a} \right)^2; \quad (4.8)$$

in the $a \rightarrow \infty$ limit, where c_1 and c_2 are positive constants depending on i . By substituting these expressions into Eq. (4.1), we can show that

$$q_+ (a) \rightarrow \frac{c_2^2}{3} (a^i); \quad (\text{for } i = 1); \quad (4.9)$$

Thus, q_+ and q_- satisfy the appropriate boundary condition.

As a bonus, we also find that

$$q (a) > 0; \quad (\text{for } i = 1); \quad (4.10)$$

Here, we show that the expression (4.1) can also be derived by considering the relation between the gauge invariant variable q and A in the synchronous gauge, which we refer to as $q_s (a)$. Here we note that we used the synchronous gauge in solving the background equations. Considering the case in which q satisfies Eq.(2.14) for $j = 0$, i.e., $q^{(0)} = (U - 3)q$, we give a gauge invariant representation of q in terms of the original variables. Since the gauge transformation $A \rightarrow A + \phi$ acts on $O(4)$ -symmetric perturbations as

$$q_A = - ; \quad q_s (a) = - - ; \quad (4.11)$$

we find that

$$\frac{a^2}{3} - A \frac{d}{d} - - ; \quad (4.12)$$

is a gauge invariant combination. By using the expressions in the Newton gauge (2.11), we can verify that this is the gauge invariant expression of q in terms of the original variables. Henceforth, we finally find that q is related to q_s as

$$q = \frac{a^2}{3} - q_s - - : \quad (4.13)$$

B. number of nodes of x

We develop a method to count the number of nodes of $x = (-q)$, where q is defined by Eq. (4.1). For the convenience, we use x instead of q , but the number of nodes of x equals to that of q if $-$ stays positive.

Proposition 5: As i is varied along (C) , the number of nodes of $x(\cdot)$ (existing between 0 and π excluding the point $= 0$) changes only when $x(i) = - (0)q(i; 0) = 0$.

Proof. It is sufficient to prove that the location of a zero point of $x(\cdot)$ should change continuously when i is swept. To show this, we suppose the opposite case. If a zero point of $x(\cdot)$ suddenly appeared at a point $= c$ other than $= 0$, $dx = d$ would have to vanish there due to the continuity of $x(\cdot)$ with respect to i . Except for the case that $-$ vanishes at $= c$, the conditions that $q(c) = q(c) = 0$ imply $q = 0$, and hence $x = 0$ because q satisfies a regular second order differential equation. Hence, the remaining possibility is that $-$ vanishes at $= c$. Then, let us examine the power series solution of q around the singular point c . Near the singularity, the behavior of 0 is given by $c(0, c)$, where c is the value of corresponding to $= c$, and c is a constant. Then, the potential U with $= 0$ in Eq.(2.14) behaves as $U = 2 = (0, c)^2$. Hence, the point $= c$ is a regular singular point, and the exponents are 1 and 2. Thus, we find that the general power series solution for x around this singular point is given by $-q = c_1(1 + \dots) + (c - c)^3 + \dots$, where c_1 and c_2 are constants. Since the case $x(c) = 0$ is considered, c_1 must be zero. Therefore, x must change its signature at $= c$. Hence $= c$ cannot be the first point at which the zero point suddenly appeared. \square

To represent the condition $x = 0$ in terms of the directions of C ,

$$(', ') = \frac{d}{d^i}; \frac{d}{d^i}; \quad (4.14)$$

we first calculate ' as

$$' = a^3 \frac{d}{1 + a^2 \frac{1}{2} A} = - \frac{a^5}{2} \frac{dV(\cdot)}{d}; \quad (4.15)$$

where we used Eq.(2.4) with $H = 0$. From this equation, we can express ' as a function of ' and '. Substituting this into Eq. (4.1), we obtain

$$x = \frac{1}{3a} \frac{d}{1 + a^2 \frac{1}{2} A} - \frac{a^3}{2} \frac{dV(\cdot)}{d}, \quad a^3 \neq 0; \quad (4.16)$$

By using Eq. (3.2), we find the above equation can be written as

$$x = \frac{a^2}{3} \frac{\theta}{\theta'} + \frac{\theta}{\theta'} = \frac{a^2}{3} \frac{d}{d^i}; \quad (4.17)$$

For the convenience, using the (\cdot, \cdot) -coordinate introduced at the end of Sec. III, we define angles $+$ and $-\$ by

$$(\cos \theta; \sin \theta) = \frac{\frac{d}{d^i}; \frac{d}{d^i}}{\frac{d}{d^i}^2 + \frac{d}{d^i}^2}; \quad (4.18)$$

along C_+ and C_- , respectively. Here, $(+ (\cdot, +))$ and $(- (\cdot, -))$ represent points corresponding to $(+ (\cdot, +))$ and $(- (\cdot, -))$ in the (\cdot, \cdot) -coordinate, respectively. To remove the ambiguity in modulo 2, we set $+(\cdot, +) = 0$ and $(\cdot, -) = \pi$.

When the curves C and (C_+) start from the vacua, both $q(\cdot)$ and $q(\cdot)$ have no node, the proof of which is presented in the appendix. Furthermore, in the limit, it is easy to see $-(> 0)$, and $q(> 0)$ was shown in Eq. (4.10). Combining these facts, we find that both x_+ and x_- are also positive when the curves C and (C_+) start from the vacua. Then $+$ and $-$ are defined without any ambiguity by choosing them to be continuous along the curves (C) with the condition that

$$0 < \theta < \pi; \quad (\text{for } i \neq 0); \quad (4.19)$$

In terms of θ , the point at which the number of nodes of q changes is specified by $\theta = n\pi$, where n is an integer.

To determine whether the number of nodes increases or decreases at a point with $\theta = n\pi$, we examine the signature of x . It is calculated from Eq. (4.1) with the aid of Eqs.(2.5) and (4.3) as

$$x = \frac{d}{1 + a^2 \frac{1}{2} A} \frac{1}{\theta}; \quad (4.20)$$

where we used $x = 0$. Then, from Fig. 2(b), we find x is positive when the curve C or (C_+) touches a constant curve with its direction pointing in the $-$ direction. By comparing this with Eq.(4.18), the defining equation of θ , we find that x is positive when $\theta = 2n\pi$, while x is negative when $\theta = (2n+1)\pi$, where n is an integer. To summarize, we have

$$\begin{aligned} \text{sgn}x &= \text{sgn} \frac{d}{d^i} = \text{sgn}(\sin \theta) \\ \text{sgn}x &= \text{sgn} \frac{d}{d^i} = \text{sgn}(\cos \theta); \end{aligned} \quad (4.21)$$

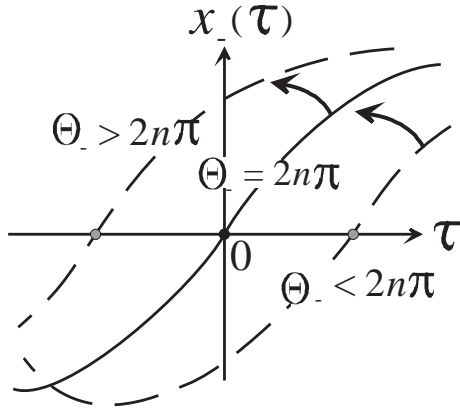


FIG 3. The behavior of $x(\tau)$ when $\Theta(\tau) > 2n\pi$. In this case, since $x > 0$, the zero point of $x(\tau)$ moves left as τ increases.

Proposition 6: we refer to the number of nodes of $x(\tau)$ as N . Then N is determined by

$$N < (N + 1): \quad (4.22)$$

Here we do not count a zero point at $\tau = 0$ as a node even if it exists.

Proof. Let us consider the $\tau < 0$ side. When $\Theta(\tau) < 2n\pi$, $x(\tau)$ changes its signature from $-$ to $+$ for increasing τ . Remember that $x > 0$ in this case. Then, it will be easy to see from Fig. 3 that the number of nodes, N , increases by one when $\Theta(\tau)$ crosses $2n\pi$ in its increasing direction. When $\Theta(\tau) > (2n + 1)\pi$, $x(\tau)$ is negative. In this case, $x(\tau)$ changes its signature from $+$ to $-$ for increasing τ . Then, again the number of nodes, N , increases by one when $\Theta(\tau)$ crosses $(2n + 1)\pi$ in the increasing direction. For the $\tau > 0$ side, we can also give an analogous discussion. Using the fact that q_j is nodeless when the curves C start from P with $0 < \Theta_j < \pi$ (See appendix), the proof is completed. \square

Now, we are ready to assign a number N for each intersection point. We define N by the relation,

$$N < (N_+ + N_-) = (N + 1): \quad (4.23)$$

Since both N_+ and N_- must be positive, we have $N > 0$. Thus we obtain

Proposition 7:

$$\Theta_j > 0; \quad \text{and} \quad N_j = 0: \quad (4.24)$$

C. a Proof of the Theorem 1

In this subsection, we give a proof of Theorem 1. We assume Θ_j stays positive throughout this subsection.

First, we explain the fact that the number of negative modes at an intersection point P is not simply given by the sum of numbers of nodes of q_j , i.e., $N_- + N_+$. In order to obtain the number of negative modes, the information about N_+ and N_- must be supplemented with the knowledge of the signature of

$$B = \frac{q_+}{q_-} - \frac{q_-}{q_+}: \quad (4.25)$$

Proposition 8: The number of negative modes is given by

$$\begin{aligned} N_- + N_+ + 1; & \quad \text{for } B > 0; \\ N_- + N_+; & \quad \text{for } B \leq 0; \end{aligned}$$

Proof. We define q_j by the solution of Eq. (2.14) that satisfies regular boundary conditions imposed at one boundary $\tau = 0$. Then, the quantity corresponding to B can also be defined for $j \neq 0$ by replacing q_j with q_{-j} in (4.25). We denote it by $B(-j)$. In the present case, the potential U is non-singular. Then, if we gradually decrease j , $B(-j)$ also decreases monotonically until it diverges to $-\infty$. When $B(-j)$ diverges, either $q_+(-j)$ or $q_-(-j)$ vanishes, and hence the number of nodes changes.

In the case of $B > 0$, decreasing j from zero, $B(-j)$ vanishes at some j before the number of nodes of q_j changes. This j is the largest negative eigen value, and the corresponding eigen function still has $N_- + N_+$ nodes. Hence, the number of negative modes is $N_- + N_+ + 1$. On the other hand, when $B \leq 0$, we gradually increase j . Then, we have the first eigen mode with positive j which has $N_- + N_+$ nodes. Hence, the number of negative modes is $N_- + N_+$. \square

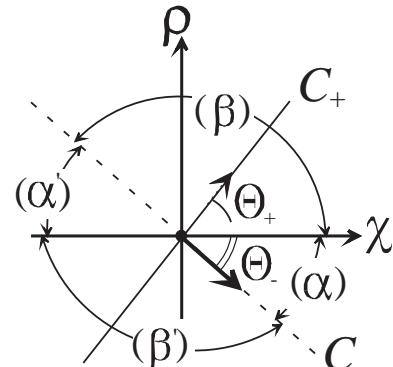


FIG 4. The diagram is rotated so that the χ -direction points rightward. For a fixed direction of the curve C , the direction of the curve C_+ is classified into four regions. The boundaries of four regions belong to the region with the smaller Θ_j .

From Proposition 8, we find that to show Theorem 1 is equivalent to show the following Proposition.

Theorem 1':

$B > 0$, $(N_+ + N_- + 1) < (\leq_+ + \leq_-)$
 $(N_+ + N_- + 2)$ (case (a)), and $B < 0$, $(N_+ + N_-) < (N_+ + N_- + 1)$ (case (b)), where case (a) includes the case in which B diverges.

Proof. We first consider which case is realized for given

. For example, we \mathbf{x} as shown in Fig.4, which is a close-up view around an intersection point in the $(\cdot; \cdot)$ -diagram as shown in Fig.2(a). This figure is rotated so as for the \cdot -direction to point rightward. Then, we classify the possible direction of the curve C_+ into four regions labeled with (\cdot) , (\cdot) , (\cdot^0) and (\cdot^0) . The boundaries of four regions belong to the region with the smaller \cdot . Then, we can see that case (a), in which $(N_+ + N_- + 1) < (\leq_+ + \leq_-) = (N_+ + N_- + 2)$, is realized when \cdot_+ is in the region (\cdot) or (\cdot^0) . To show $B > 0$ in this case, we evaluate B by using Eq. (4.15) to find

$$B = \frac{1}{q_+ q_-} \cdot \cdot_+ \cdot \cdot_- + : \quad (4.26)$$

In the regions (\cdot) and (\cdot) , the quantity in the round bracket is positive. On the other hand, the quantity $q_+ q_-$ is positive in the regions (\cdot) and (\cdot^0) . Consequently, we obtain $B > 0$ in the regions (\cdot) and (\cdot^0) . The case in which the curve C_+ is pointing upward can be discussed in the same way.

2

Remark: The value of \cdot at P does not cross \cdot under a continuous deformation of the curves C as long as the way of intersection at P is unchanged and the curves do not cross the points O , P_+ and P_- . Hence, the number N at a point P is invariant under such a continuous deformation of C .

V. MULTIPPLICITY OF WALLS

From our method to find solutions from the intersection points of two curves C , the solution may have several nodes of \cdot . We show this number of nodes, M , can also be read from the $(\cdot; \cdot)$ -diagram.

For this purpose, we prove the following statement.

Proposition 9: A point where $\cdot(\cdot^i) = 0$ appears only from the boundary specified by $\cdot = 0$, as we vary i along the curves C .

Proof. Let us assume that a point at which $\cdot(\cdot^i; \cdot) = 0$ appeared at an intermediate point $\cdot = s \neq 0$ abruptly. Then, we must have $\cdot(\cdot^i; s) = 0$ from the continuity of $\cdot(\cdot^i; s)$ with respect to both i and s . However, the old equation (2.5) indicates that $dV/d\cdot = 0$ at this

point. Then, this solution must be one of the trivial solutions $\cdot = 0$, which correspond not to an intermediate point of C but to their end points. This is a contradiction. 2

Theorem 2:

The number of nodes of $\cdot(\cdot)$ for a solution corresponding to an intersection point P is given by

$$M = (\cdot_+ + \cdot_-) = \cdot_{at P} : \quad (5.1)$$

Proof. From Proposition 9, the number of nodes of $\cdot(\cdot^i; \cdot)$ changes only when $\cdot(\cdot^i) = 0$ as we change i along the curves C . This happens if and only if $\cdot = m$ where m is an integer. Denote by M the number of nodes of \cdot (existing between 0 and \cdot excluding the point $\cdot = 0$). To avoid duplicative counting, we do not count the point $\cdot = 0$ as a node when $\cdot(0) = 0$ but we count it as a node when $\cdot_+(0) = 0$. Here we use the same technique that was used to count the number of nodes of \mathbf{x} in the subsection IV B. Corresponding to Eq.(4.20), the derivative of \cdot with respect to \cdot at $\cdot = 0$ is calculated as

$$\frac{d}{d\cdot} \cdot_{\cdot = 0} = \frac{dV}{d\cdot} (\cdot); \quad (\text{when } \cdot = 0) : \quad (5.2)$$

This quantity is positive (negative) when \cdot is negative (positive). Then, for the same reasoning as was used to determine the number of nodes for \mathbf{x} , we find the relations,

$$\begin{aligned} M & \cdot 1) < M ; \\ M_+ & \cdot_+ < (M_+ + 1) : \end{aligned} \quad (5.3)$$

For an intersection point, (\cdot) is given by $\cdot < 0$ and $\cdot_+(\cdot)$ for $\cdot > 0$. Thus, the number M , which is the total number of nodes of $\cdot(\cdot)$, is given by $M_+ + M_-$. Then, from Eq.(5.3), we find $(M - 1) < \cdot_+ < (M + 1)$. Since \cdot_+ must be deviated by 2, we finally find M is given by (5.1). 2

Remark: Theorem 2 tells that $M = 2$ is the winding number around O of the continuous curve $P_+ P_- P$, that is obtained by connecting P_+ ; P and P_- with C_- and C_+ . Thus, the number M is invariant under a continuous deformation of curves C as long as the curves do not cross the points O , P_+ and P_- .

V.1. COMPARISON OF THE VALUES OF ACTIION BETWEEN VARIOUS BOUNCE SOLUTIONS

We introduce a pseudo-action defined as a function of i and \cdot_+ by

$$S_E(\cdot_+^i; \cdot^i) = S_+(\cdot_+^i) + S_-(\cdot^i); \quad (6.1)$$

and

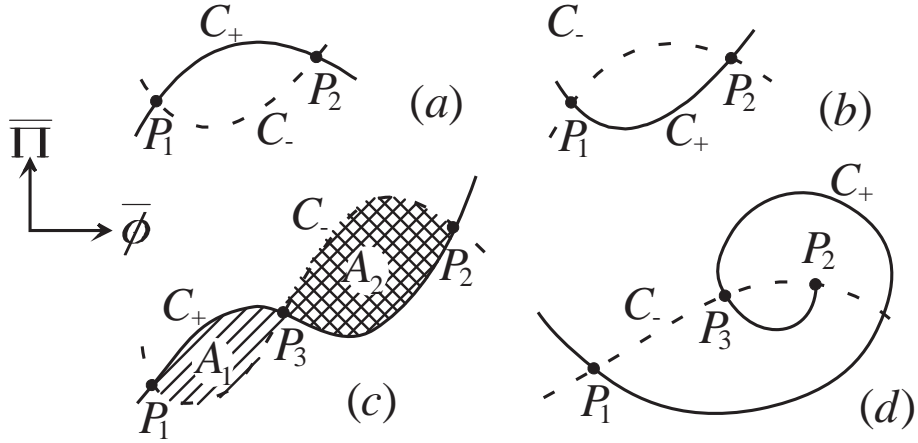


FIG. 5. A few examples to show various ways of connection between two intersection points P_1 and P_2 . It is possible to compare the values of action from this diagram, as explained in the text. We can show that $S_E[P_1] > S_E[P_2]$ for case (a), $S_E[P_1] < S_E[P_2]$ for case (b), $S_E[P_1] < S_E[P_2]$ if $A_1 < A_2$ for case (c), and $S_E[P_1] < S_E[P_2]$ for case (d).

$$S(\dot{a}) = \int_0^Z d\dot{a} L[a(\dot{a}); \dot{a}]; \quad (6.2)$$

where

$$L[a] = a^3 \frac{1}{2} \dot{a}^2 + V(a) - \frac{3}{a} \frac{\dot{a}^2}{a^2} + \frac{1}{a^2} \quad : \quad (6.3)$$

Note that $S(\dot{a})$ is defined along the curve C , and hence so S_E is. To the contrary, the original action S_E is well-defined only at intersection points which represent CD bounce solutions. For CD bounce solutions, i.e., at intersection points, we have $S_E = S_E$.

Then, we calculate

$$\begin{aligned} \frac{dS}{d\dot{a}} &= \int_0^Z d\dot{a} \frac{\frac{\partial L}{\partial \dot{a}}}{a} \frac{\partial a}{\partial \dot{a}} \\ &+ \frac{\frac{\partial L}{\partial \dot{a}}}{\partial \dot{a}} \\ &+ \frac{6}{a} \frac{\partial a}{\partial \dot{a}} + a^3 - \frac{\partial}{\partial \dot{a}} \\ &+ \frac{d(\dot{a})}{d\dot{a}} L[a; \dot{a}] = \\ &= 2^2 \quad ; \end{aligned} \quad (6.4)$$

where partial differentiations with respect to \dot{a} are taken for fixed a , and we used the fact $(\dot{a}; a)$ satisfies the background equations, i.e.,

$$\begin{aligned} \frac{L}{a} &= \frac{d}{d\dot{a}} \frac{\partial L}{\partial a} + \frac{\partial L}{\partial a} = 0; \\ \frac{\partial L}{\partial a} &= \frac{d}{d\dot{a}} \frac{\partial L}{\partial \dot{a}} + \frac{\partial L}{\partial \dot{a}} = 0; \end{aligned} \quad (6.5)$$

Integrating this expression, we find that the difference of the values of action between two bounce solutions specified by points P_1 and P_2 is given by

$$S_E[P_2] - S_E[P_1] = \int_{P_1}^{P_2} d\dot{a} (\dots) \quad (6.6)$$

When the two curves connecting P_1 and P_2 do not intersect with each other, the signature of $S_E[P_2] - S_E[P_1]$ is totally determined by the topological information of

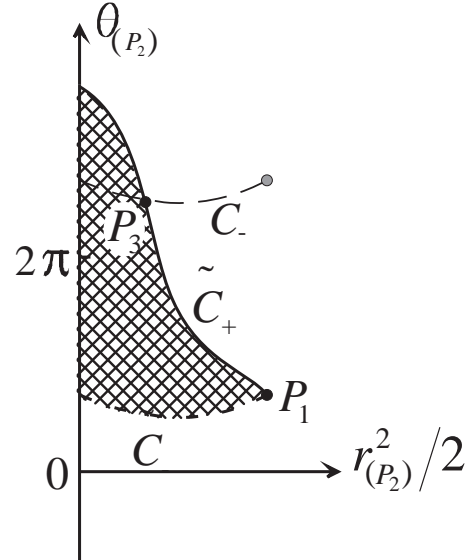


FIG. 6. A plot of C connecting P_1 and P_2 in the spherical coordinate $(r_{(P_2)}, \theta_{(P_2)})$ centered at P_2 . In this coordinate C has many copies in this coordinate. We specify one pair of curves by the condition that the point P_1 exists in the region $0 < \theta_{(P_2)} < 2\pi$. We attach \sim to these specific curves as C^\sim to distinguish them from other copies. Then, in this coordinate, the area surrounded by C_+ and C_- gives the difference of the values of action at P_1 and P_2 .

the connecting curves. As shown in Fig.5(a), if the region surrounded by the two curves is on the left hand side when we move from P_1 to P_2 along the curve C , $S_E[P_1] > S_E[P_2]$ can be concluded. The difference is proportional to the area surrounded by the two curves. In the opposite case as shown in Fig.5(b), we can say $S_E[P_1] < S_E[P_2]$. In such a case as presented in Fig.5(c), we need to compare the areas A_1 and A_2 to determine which point has the smaller value of action. In some cases, however, even when there is another intersection point between P_1 and P_2 as shown in Fig.5(d), we can determine which point has the smaller value of action from the topological information alone. In the case of Fig.5(d), we can say that $S_E[P_1] < S_E[P_3]$ and $S_E[P_3] < S_E[P_2]$. Hence $S_E[P_1] < S_E[P_2]$ is concluded.

For our present purpose, we do not have to give a general statement in what situation we can determine the signature of $S_E[P_2] - S_E[P_1]$ from the topological information alone. Only the case discussed below is of special importance. Let us draw the two curves C by using a spherical coordinate $(r_{(P_2)}, \theta_{(P_2)})$ whose origin is located on P_2 , i.e., the point P_2 corresponds to the line $r_{(P_2)} = 0$. In this coordinate, when the value of $\theta_{(P)}$ of two points are different by 2π with an integer n , these two points are identical on the original (θ, ϕ) -plane. Thus, there are many copies of the curves C in the $(r_{(P_2)}, \theta_{(P_2)})$ -coordinate. We choose one pair of C both of which pass through a common point corresponding to P_1 in the $(r_{(P_2)}, \theta_{(P_2)})$ -coordinate, and denote them by C' . If we choose this point, say, to satisfy P_1 with $0 < \theta_{(P_1)} < 2\pi$, the two curves C' can be drawn without any ambiguity. If the two curves C' do not intersect between P_1 and P_2 in this coordinate as shown in Fig.6, where we used $r_2^2 = 2$ as the horizontal coordinate instead of r_2 , the $(S_E[P_2] - S_E[P_1]) = 2$ is given by the area of the shaded region, and we can say it is positive. We note that no

intersection in this coordinate does not mean no intersection on the original (θ, ϕ) -plane. In fact, Fig.6 represents the same situation that was shown in Fig.5(d).

The result obtained in this section is summarized by the following Theorem.

Theorem 3:

We choose one pair of C such that they pass through a common point corresponding to P_1 in the $(r_{(P_2)}, \theta_{(P_2)})$ -coordinate, and denote them by C' as shown in Fig.6. If these two curves does not intersect between P_1 and P_2 and if the value of $\theta_{(P_2)}$ at $r_{(2)} = 0$ on C'_+ is larger than that on C'_- , then $S_E[P_1] < S_E[P_2]$.

Remark: Theorem 3 depends only on the topological information about intersections between the curves C'_+ and C'_- . Hence, we can apply the same statement for any deformed diagram which preserves this topological information.

VII. A PROOF OF THE "NO-NEGATIVE MODE THEOREM"

Now, we prove the Main Theorem (the "no-negative mode theorem"). Namely, we prove if an intersection point P has either negative modes or nodes of $-(\cdot)$, there exists another intersection point P^0 which has a smaller value of action than P . By using Theorem 1 given in Sec.IV and Theorem 2 given in Sec.V, the Main Theorem is reduced to the following statement.

The Main Theorem':

The intersection point with $N \neq 0$ or $M \neq 0$ cannot be the solution that realizes the minimum value of action.

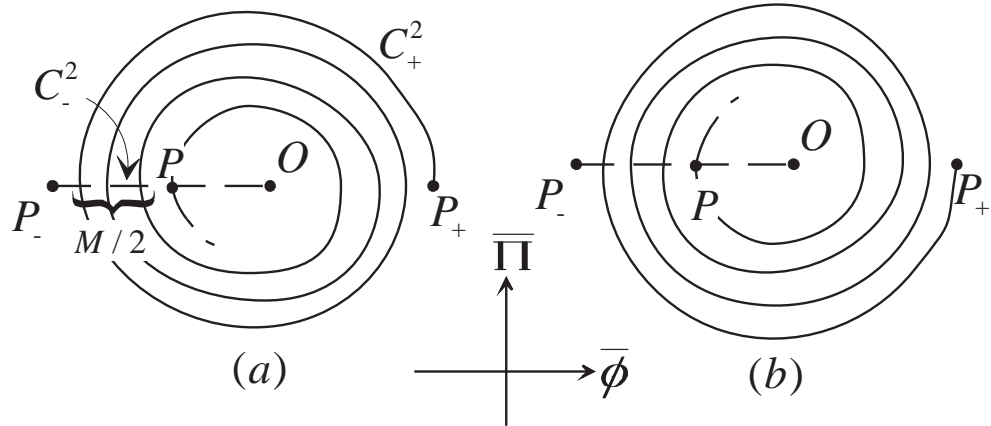


FIG.7. Under the constraint that the curves do not cross the points O , P_+ and P_- , the deformed diagram D^2 consisting of C^2 can be reduced to one of these two diagrams. However, we can see that $M < 0$ for the point P in the diagram (b). As we know $M \neq 0$, the possibility (b) is removed. In the diagram (a), the winding numbers $M = 2$ can be zero.

To show the above statement, we first define curves C^1 by deforming C continuously to make C to be a straight line connecting P_+ and O . Under this deformation of curves, the way of intersections, i.e., the value of $\gamma_{+} + \gamma_{-}$ at each intersection point, is kept unaltered, and the curves do not cross the points O , P_+ and P_- . The diagram composed of these deformed curves keeps the numbers N and M assigned for each intersection point, and also it still keeps some information about the difference between the values of action for different points. In fact, under the situation such that Theorem 3 determines which point has the smaller value of action, we can apply the Theorem to this deformed diagram in place of the original one. We denote this diagram consisting of C^1 by D^1 .

Focusing on a point P in D^1 , we further deform C_+^1 continuously. Under this deformation, we allow the way of connections at points other than P to change, and hence the number of intersection points can be varies. Furthermore, we allow the value of γ at P to deviate from $\gamma_{(P)}$, where $\gamma_{(P)}$ is the original value of γ at P . However, we do not allow the curve to cross the points O , P_+ and P_- . Hence, the number M for P is kept unaltered. Then, the diagram can be reduced to the diagram that are shown in Fig.7(a). The cases given by Fig.7(b) are not realized because the number M for the point P becomes negative. We denote these further deformed curves by C^2 (c.f., $C^2 = C^1$) and the corresponding diagram by D^2 . As noted in the previous section, the number M represents twice the number of windings of the curve $P_+ P P_+$ around O .

Now we use the $(r_{(P)}, \theta_{(P)})$ -coordinate introduced in Sec.VI. In this coordinate, the curves have many copies. As before, we attach \sim to a specific pair of curves to distinguish it from others. It is explained below how we select the specific curves. The deformed diagram D^2 in this coordinate is given by Fig.8(a) when $M \neq 0$ and by Fig.8(b) when $M = 0$. In both cases, C_+^2 and C_-^2 are shown by the thick rigid line and by the thick dashed line, respectively. Here, P_n in Fig.8(a) is the intersection point neighboring to P in Fig.7(a). Later, we consider the process that the diagram D^1 is recovered from D^2 through continuous deformation of curves. In the midst of this process, we use the notation C^* to specify the curves that are denoted by C^2 in the diagram D^2 . We refer to the point corresponding to the point P on the curve C_+ by $P_{(+)}$, (Do not be confused with P_+ !) and we denote the value of $\gamma_{(P)}$ at $P_{(+)}$ by $\gamma_{(+)}$. In both case (a) and case (b), we choose C_+^2 so as to satisfy $0 < \gamma_{(+)} < \gamma$. The part of the curve C^2 connecting P_+ and P_- is given by the lines with $\theta_{(P)} = (2n-1)\pi$, where n is an integer. We choose the line with $n=0$ as C^2 for case (a), and that with $n=1$ for case (b). They are presented by the thick dashed lines in Fig.8.

Proposition 10: We consider the diagram D^1 that is recovered from the diagram D^2 given in Fig.8(a) or (b). For this diagram, $[\gamma_+ = \gamma_-]$ is given by $[\gamma_{(P)} = \gamma]$, where $\gamma_{(P)}$ is the value of γ at P in the original diagram. (Here we denoted the largest integer less than or equal to x by $[x]$.) Furthermore, γ_+ in the diagram D^1 must be greater than 0.

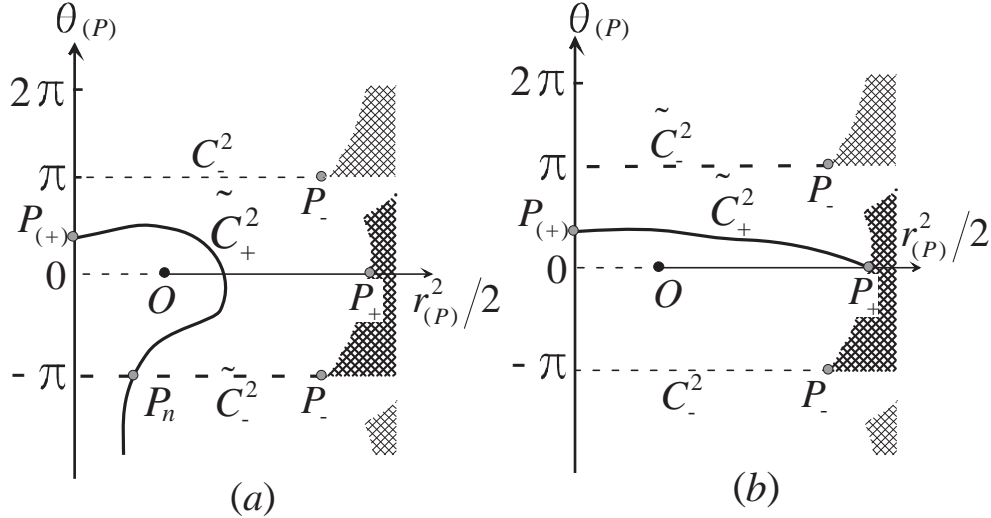


FIG.8. (a) The distorted diagram D^2 in the $(r_{(P)}, \theta_{(P)})$ -coordinate corresponding to Fig.7(a) when $M \neq 0$. The curve C_+^2 is shown in from P in the direction for P_+ . The shaded region corresponds to the forbidden regions labeled with () and () in Fig.2(b). P_n is the intersection point neighboring to P in D^2 . (b) The same diagram when $M = 0$.

Proof. From Fig.7(a), one can see that the value of P for this deformed diagram D^2 is also in between 0 and $+$. Hence, we find $[+]=[-]$ for the diagram D^2 . In recovering the diagram D^1 from D^2 , the direction of the curve C_+^2 in Fig.7(a) may rotate around P . Under this reordering, both $+$ and $-$ increase when the direction of C_+ rotates in the anti-clockwise direction, and both of them are divided by when C_+ becomes parallel to C_- at P . Hence, we can say that the relation $[+]=[-]$ is maintained under the deformation from D^2 to D^1 . Therefore, when the diagram D^1 is recovered, the point $P_{(+)}$ is moved along the (P) -axis to a point satisfying $[P_{(+)}]=[-]=0$. The latter part of the Proposition is manifest from Proposition 7, which tells (P) must be positive. \square

Theorem 4:

A point P with $M \neq 0$ cannot be the solution that realizes the minimum value of action.

Proof. Let us consider the continuous deformation of curves to recover the diagram D^1 from D^2 in the $(r_{(P)}; (P))$ -coordinate. As shown in Fig.8(a), C_+^2 has an intersection point P_n with C^2 ($= C^1$). From the continuity of deformation, the curve C_+^1 , as well as C_+^2 , must intersect with C^1 . Then, let us refer to the first intersection point nearest to P as P^0 . Since the curve C_+^1 does not intersect with the curve C^1 between P and P^0 by definition, the area surrounded by these two curves connecting P and P^0 has a definite signature. By virtue of Proposition 10, $P_{(+)}$ in the diagram D^1 must be on the upper side of the $(P) = 0$ line. Hence, by using Theorem 3, we conclude $S_E [P^0] < S_E [P]$. \square

Theorem 5:

A point P with $N \neq 0$ and $M = 0$ cannot be the solution that realizes the minimum value of action.

Proof. Again, we consider the continuous deformation to recover the diagram D^1 from D^2 in the $(r_{(P)}; (P))$ -coordinate. In the case $M = 0$, the diagram D^2 is given by Fig.8(b). If $N > 1$, (P) must be greater than 0 . Then, owing to Proposition 10, $+$ for the diagram D^1 must be greater than 0 . Consequently, we find that the point $P_{(+)}$ moves to the upper side of the $(P) = 0$ line, while the point P_+ must stay on the opposite side. Recalling the forbidden region shown as shaded regions in Fig.8(b), we find that the curve C_+^1 must have at least one intersection point with C^1 . Let us refer to the first intersection point nearest to P as P^0 . Then, as before, we can use Theorem 3 to conclude $S_E [P^0] < S_E [P]$. \square

Now, from Theorem 4 and Theorem 5, the proof of the Main Theorem is completed.

V III. SUMMARY

We gave a proof of the "no-negative mode theorem", which tells that the bounce solution realizing the smallest value of action among all $O(4)$ -symmetric CD bounce solutions has no-negative mode and has no node in $-$. We summarize the outline of the proof presented in this paper. In Sec. III, we introduced a diagram which consists of two curves. We showed that each intersection point of these two curves corresponds to an $O(4)$ -symmetric CD bounce solution. In Sec. IV and V, we assigned two numbers N and M for each intersection point. The number N is defined by (4.23), and it was shown to represent the number of negative modes when $M = 0$. The number M is defined by (5.1), and it was shown to be the number of nodes of $-$. As is easily seen from their definitions, both N and M have a clear topological meaning. In Sec. V I, we gave a general rule to compare the values of action between different intersection points from the topological information of the diagram introduced in Sec. III. Collecting these statements related to the topology of the diagram, the "no-negative mode theorem" was proved in Sec. V II.

The "no-negative mode theorem" is known to be equivalent to the "no-supercritical supercurvature mode conjecture" [3]. Therefore, we also proved that there appears no-supercritical supercurvature mode in the one-bubble open inflation universe.

Acknowledgments

The author thanks M. Sasaki and J. Garriga for helpful discussions. This work was supported in part by Saneyoshi Scholarship.

APPENDIX A:

In this appendix, we show that $q^{(i)}()$ is positive in the i ! limit. For $i = 1$, $()$ will stay near 0 , and the geometry does not significantly differ from the de Sitter space. In both $+$ and $-$ cases, the limiting behavior of $q^{(i)}()$ is essentially same. To avoid an unnecessary complication, we discuss the false vacuum side as a representative case. Similar arguments can be repeated for the true vacuum side.

The equation for $(i) = ()$ can be approximately written as

$$+ 3H - m^2 = 0; \quad (A1)$$

where $m^2 = d^2 V() = d^2 = 0$. Since H is almost independent of $+$, Eq. (A1) reduces to a linear differential equation. Hence, in this limiting case, solutions of Eq. (A1) with different initial values of $+$ are obtained

by a simple scaling. By introducing a scaling parameter $(^i)$, is written as

$$(^i;) = (^i) _0(); \quad (A2)$$

where $_0()$ satisfies Eq.(A1). Then, we have

$$'() = \frac{d}{d^i} _0(); \quad (A3)$$

where $d = d^i$ is positive, and hence $_0() > 0$ because $'() = 1$. Substituting these approximate expressions into (4.1), we find

$$q = \frac{a^2}{3} \frac{d}{d^i} \frac{-_0^2}{m^2} m^2 - 3H - !^2; \quad (A4)$$

where $! = -_0 = _0$. Since $_0$ and $-_0$ stay non-negative in the present limiting case, we have $! = 0$. Furthermore, the equation that $!$ should satisfy is given by

$$! = m^2 - 3H - !^2: \quad (A5)$$

At $! = 0$, $! < 0$. Then if $!$ became greater than m , there would be a point at which both $! = m$ and $! = 0$ are satisfied. However this is impossible from Eq. (A5). Thus, $! < m$ is maintained. Then, the condition $0 < ! < m$ with Eq.(A4) implies that q stays positive until $= 0$.

Tanaka, K. Yamamoto and J. Yokoyama, Phys. Lett. B 317, 510 (1993); Martin Bucher, Neil Turok, Phys. Rev. D 52, 5538 (1995); M. M. Bucher and N. Turok, Phys. Rev. D 52, 5538 (1995); A. Linde, Phys. Lett. B 351, 99 (1995); A. Linde and A. M. Maziuk, Phys. Rev. D 52, 6789 (1995); J. Garcia-Bellido, J. Garriga and X. Montes, Phys. Rev. D 57, 4669 (1998).

- [2] M. Sasaki, T. Tanaka and K. Yamamoto, Phys. Rev. D 51, 2979 (1995);
- [3] T. Tanaka and M. Sasaki, Phys. Rev. D (1998) in press.
- [4] T. Tanaka and M. Sasaki, Prog. Theor. Phys. 88 (1992), 503.
- [5] S. Coleman, Phys. Rev. D 15, (1977), 2929; in The Woods of Subnuclear Physics, Proceedings of the International School, Erice, Italy, ed. A. Zichichi, Subnuclear Series Vol. 15 (Plenum, New York, 1979), p. 805.
- [6] C. G. Callan, Jr. and S. Coleman, Phys. Rev. D 16, 1762 (1977).
- [7] S. Coleman, Nucl. Phys. B 298, 178 (1988); S. Coleman, V. G. Lai and A. Martin, Comm. Math. Phys. 58 (1978), 211.
- [8] S. Coleman and F. De Luccia, Phys. Rev. D 21, 3305 (1980).
- [9] P. A. M. Dirac, Lectures on Quantum Mechanics, Yeshiva University, (1964).
- [10] J. Garriga, X. Montes, M. Sasaki and T. Tanaka, Nucl. Phys. B 513, 343 (1998).
- [11] S. W. Hawking and N. Turok, Phys. Lett. B 425, 25 (1998).
- [12] A. Vilenkin, Phys. Rev. D 57, 7069 (1998).
- [13] S. W. Hawking and I. G. Moss, Phys. Lett. 110B, 35 (1982).
- [14] G. W. Gibbons, S. W. Hawking and M. J. Perry, Nucl. Phys. B 138 (1978), 141.

[1] J. R. Gott III, Nature 295, 304 (1982); J. R. Gott III and T. S. Statler, Phys. Lett. 136B, 157 (1984); M. Sasaki, T.